Pharmaceutical Research, Vol. 22, No. 4, April 2005 (© 2005)
10.1007/s11095-005-2503-0

Research Paper

High-Performance Frontal Analysis of the Binding of Thyroxine Enantiomers to Human Serum Albumin

Tomoko Kimura,[1] Keiko Nakanishi,[1] Terumichi Nakagawa,[2] Akimasa Shibukawa,[3] and Katsumi Matsuzaki[1,4]

Received October 14, 2004; accepted December 15, 2004

Purpose. The aim of this study was to characterize the binding property between thyroxine and human serum albumin (HSA) qualitatively and enantioselectively using high-performance frontal analysis (HPFA).
Methods. An on-line HPLC system consisting of an HPFA column, an extraction column, and an analytical HPLC column was developed to be used to determine the unbound concentrations of thyroxine enantiomers.
Results. Both enantiomers were bound to human serum albumin at two high-affinity sites with similar affinities. The binding constant (K) and the number of binding sites on an HSA molecule (n) evaluated from Scatchard plot analysis were $K = 1.01 \times 10^6$ M-1 and n = 1.90 for L-thyroxine, and $K = 9.71 \times 10^5$ M-1 and n = 1.97 for D-thyroxine. The binding sites were identified using phenylbutazone and diazepam as site-specific probes for sites I and II, respectively, and each enantiomer was found to bind to both sites. Incorporation of a chiral HPLC column into the on-line system permitted the investigation of enantiomer-enantiomer interactions, which revealed that both enantiomers competitively bind to the same binding sites without significant allosteric effects.
Conclusions.

KEY WORDS: albumin; enantiomer; high-performance frontal analysis; HPLC; protein binding; thyroxine.

INTRODUCTION

After introduction into the systemic circulation, exogenous and endogenous compounds undergo some degree of reversible binding to plasma proteins including albumin, α1-acid glycoprotein, and lipoproteins. Plasma protein binding controls the distribution, excretion, and activity of drugs (1,2). Therefore, the investigation of protein binding properties in the plasma is a central issue to drug development and safety for clinical use.

On the other hand, the plasma protein binding of endogenous compounds such as hormones has not been intensively and widely investigated. However, plasma protein binding affects the biological activities of several hormones such as for familial dysalbuminemic hyperthyroxinemia, which is caused by a mutation in the human serum albumin (HSA) gene, resulting in 10-fold stronger binding affinity (3).

Thyroxine (3,3′,5,5′-tetraiodothyronine; T4) is a thyroid hormone that strongly binds to plasma proteins such as albumin, thyroxine-binding globulin, and transthyretin. As shown in Fig. 1, T4 is a chiral compound that contains an asymmetric carbon atom and a pair of T4 enantiomers that exhibit different biological activities. The naturally occurring form of this thyroid hormone is L-(–)-thyroxine (L-T4), which physiologically regulates a number of biological processes including oxygen consumption, protein synthesis, carbohydrate metabolism, growth and development, and the maintenance of body weight. In contrast, D-(+)-thyroxine (D-T4) has marked cholesterol level reducing activity but does not affect the basal metabolic rate (4–6).

Human serum albumin (HSA) is the most abundant protein found in human plasma and has two principle binding sites: a warfarin site (site I) and a benzodiazepine site (site II). A wide variety of drugs and endogenous compounds including thyroxine are bound to HSA. The administration of drugs or accumulation of endogenous compounds that share the same binding site with thyroxine may increase the unbound T4 concentration, resulting in unexpected changes in its physiologic activity (7) and its elimination. Therefore, quantitative and competitive binding studies focusing on the evaluation of binding parameters and identification of binding sites would be of practical benefit.

Thus far, the parameters for binding between L-T4 and HSA have been evaluated by several groups using equilibrium dialysis (8), fluorescence quenching (9), and enzymatic methods (10). However, discrepancies in the results were found for the number of high-affinity binding sites (n), where some studies reported n = 1 (8,9), whereas others reported n = 2 (11). Hage and co-workers investigated T4-HSA binding

[1] Graduate School of Pharmaceutical Sciences, Kyoto University, Sakyo-ku, Kyoto, 606-8501, Japan.
[2] Faculty of Pharmaceutical Sciences, Setsunan University, 451 Nagao tiuge-cho Hirakata, 573-0101, Japan.
[3] Faculty of Pharmaceutical Sciences, Chiba Institute of Science, Chosi, 288-0025, Japan.
[4] To whom correspondence should be addressed.

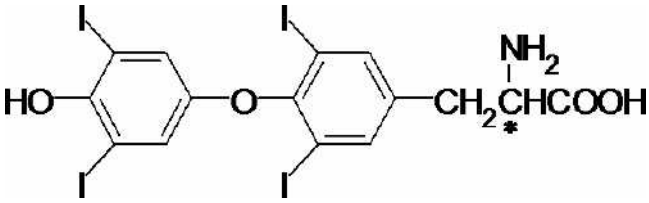

Fig. 1. Chemical structures of tyroxine (T4). The asterisk indicates the asymmetric carbon.

using an HSA-immobilized HPLC column, and found that T4 enantiomers bind at sites I and II (12). However, the binding site of nonimmobilized HSA has not been identified. In addition, the effects of enantiomer-enantiomer interaction on T4-HSA binding have not been investigated.

High-performance frontal analysis (HPFA) is a chromatographic method suitable for the analysis of strong drug-protein binding and has several unique features associated with it (13–15). HPFA is free from the undesirable effects of conventional methods such as for ultrafiltration and dialysis such as adsorption onto or leakage from the membrane. In addition, it can be easily incorporated into an on-line HPLC system. On-line coupling with a chiral HPLC column allows for stereoselective binding analyses, and coupling with a preconcentration column enhances detectability. To date, HPFA has been used for sensitive analyses of strong plasma protein bindings (bound fraction >99%) and in enantioselective protein binding studies of several chiral drugs. However, HPFA has not been applied in binding studies of endogenous compounds.

In this study, HPFA was applied to examine the quantitative and competitive binding between HSA and T4 enantiomers. The binding parameters of the enantiomers were evaluated by Scatchard plot analysis, and the binding sites were identified by means of a competitive binding study using phenylbutazone and diazepam as site-specific probes for sites I and II, respectively. In addition, the enantiomer-enantiomer interaction of T4 upon HSA binding was investigated. HPFA is useful for investigating binding properties that are often difficult to elucidate by conventional methods involving binding analysis. This is the first report of the application of HPFA method to study the binding of an endogenous compound.

MATERIALS AND METHODS

Materials and Apparatus

L-Thyroxine sodium salt and D-thyroxine sodium salt were purchased from Wako (Osaka, Japan), and HSA (cat. no. A-1887, fatty acid free) and dizaepam were purchased from Sigma (St. Louis, MO, USA). Phenylbutazone was supplied by Nakalai Tesque (Kyoto, Japan). All sample solutions were prepared in sodium phosphate buffer (pH = 7.4, I = 0.17). Develosil 100 Diol 5 was acquired from Nomura Chemicals Co. (Seto, Japan), ODS-AM YMC-Pack was from YMC (Kyoto, Japan), and ULTRON ES-OVM was from Shinwa Chemicals Co. (Kyoto, Japan).

On-line HPFA/HPLC System

Figure 2 shows a schematic of the on-line HPLC system used in this study, where a HPFA column, extraction column, and analytical column were connected via a four-port switching valve and a six-port switching valve. The setup consisted of LC 9A and LC 10AS HPLC pumps (Shimadzu, Kyoto, Japan), SPD-10A UV detectors (Shimadzu), a Rheodyne Type 8125 injector, a chromatopac C-R8A integrated data analyzer (Shimadzu), and a CS-300C column oven (Chromato-Science, Osaka, Japan).

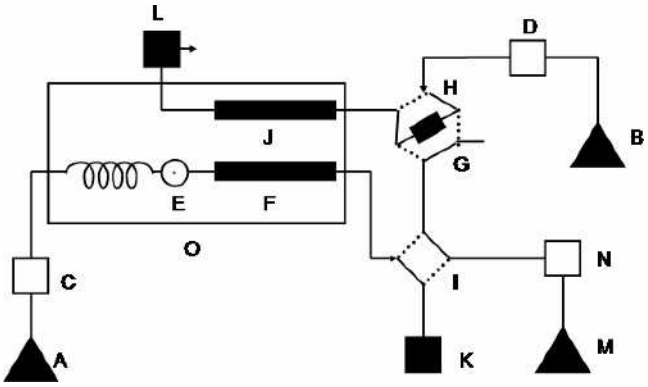

Fig. 2. Schematic diagram of on-line HPFA/HPLC system. (A) Mobile phase for HPFA; (B) mobile phase for analytical column; (C and D) pump; (E) sample injector; (F) HPFA column; (G) six–port valve; (H) extraction column; (I) four-port valve; (J) analytical column; (K and L) UV detector; (M) distilled water to extraction column; (N) pump; (O) column oven.

Table I lists the HPLC conditions used to obtain data for the Scatchard analysis of T4-HSA binding. Physiologic pH (7.4) sodium phosphate buffer was used as the mobile phase for HPFA without the addition of an organic modifier so not to disturb the binding equilibrium. A hydrophilic HPFA column composed of diol-silica was selected so that hydrophobic T4 enantiomers and two competitive drugs could be eluted even under mild mobile phase conditions.

Determination of Unbound Drug Concentrations by HPFA/HPLC System

After 1.3 ml of sample solution was directly injected into the HPFA column, T4 was eluted out as a zonal peak with a plateau region. According to the principle of high-performance frontal analysis (13), the T4 concentration in this plateau region was equal to the unbound T4 concentration in the sample solution. A 1.3 ml volume of this plateau region was then transferred into the extraction column by switching the four-port valve via the "heart-cut" procedure, after which the unbound T4 was trapped on the extraction column. Next, the mobile phase for the analytical column was introduced into the extraction column by switching the six-port valve so as to transfer the trapped T4 into the analytical column. The extraction column was then washed with distilled water for 30 s before and after the heart-cut procedure. The HPFA column and the analytical column were kept at 37°C in a column oven at all times during this procedure.

The sample solution loaded in the injector loop was injected into the HPFA column without sample diffusion in the sample loop so that the binding equilibrium was not disturbed so to prevent the plateau region from disappearing. The "injector-reswitching technique" was helpful in overcoming this problem as follows (16). The injector loop was loaded with a 1.3 ml volume of the sample solution connected to the mobile

Table I. HPFA Conditions

Subsystem	Condition	
HPFA	Column	Develosil 100-Diol-5 (5 cm × 4.6 mm i.d.) (1)(2)(4)(6) Develosil 100-Diol-5 (15 cm × 6 mm i.d.) (3)(5)
	Mobile phase	Sodium phosphate buffer (pH 7.4, I = 0.17)
	Flow rate	1.0 ml/min
	Extraction column	Develosil ODS 10 (1 cm × 4.6 mm i.d.)
Analytical HPLC	Column	YMC-Pack ODS-AM (15 cm × 4.6 mm i.d.)(1)–(5) ULTRON ES-OVM (15 cm × 4.6 mm i.d.) (6)
	Mobile phase	Sodium phosphate buffer (pH 4.6, I = 0.04): CH_3CN = 7:3 (V:V) (1), 6:4 (V:V) (2)(3)(5), 61:39 (V:V) (4) Sodium phosphate buffer (pH 4.6, I = 0.04): EtOH = 4:6 (V:V) (6)
	Flow rate	1.0 ml/min
	Detection	UV 230 nm

(1) T4-HSA Scatchard analysis; (2) diazepam-HSA Scatchard analysis; (3) phenylbutazone-HSA Scatchard analysis; (4) the competitive study between T4 and diazepam; (5) the competitive study between T4 and phenylbutazone; (6) the study of enantiomer-enantiomer interaction upon T4-HSA binding.

phase flow at 1 ml/min for 0.8 min, and then it was disconnected from the mobile phase flow. As a result, the diffused portion of the sample solution in the loop was not introduced into the HPFA column, so that the actual injection volume was 0.8 ml.

The HPLC conditions for the competitive binding studies using diazepam and phenylbutazon, and for the enantiomer-enantiomer effects on T4-HSA binding are shown in Table I. The retention of phenylbutazone onto the diol-silica column was weaker than that of diazepam, and a larger HPFA column was therefore used for the competitive binding study involving phenylbutazone to ensure proper retention. For the enantiomer-enantiomer interaction study, a chiral HPLC column was used to determine the unbound concentrations of both enantiomers. The binding constant (K) and the number of binding sites per one protein molecule (n) were then estimated according to the following equation:

$$r/Cu = -Kr + nK \quad (1)$$

where r and Cu represent the amount of bound drug per one protein molecule and the unbound drug concentration, respectively.

Scatchard Analyses of Diazepam-HSA Binding and Phenylbutazone-HSA Binding

Table I lists the HPLC conditions for the Scatchard plot analysis of diazepam-HSA and phenylbutazone-HSA binding, respectively. A series of sample solutions containing 5–80 μM diazepam or 10–80 μM phenylbutazone in 100 μM HSA was injected into the on-line HPFA/HPLC system (injection volume of 1.5 ml) to determine the unbound drug concentrations, and Scatchard plots were then made. The heart-cut time was set at 4–4.5 min for diazepam and 13.0–13.5 min for phenylbutazone, and a 10 μl volume of a series of standard solutions consisting of 2, 5, 10, 20, and 40 μM for diazepam and 10, 20, 60, 80, 100, and 225 μM for phenylbutazone in methanol were used to prepare the calibration curves, which showed good linearity (rsq. > 0.999). Further detailed analysis using nonlinear fitting of the raw data to different binding models incorporating specific and nonspecific binding was performed using Multi software. From the model regression, the optimal AIC values were then compared. The evaluated binding parameters were $K = 1.22 \times 10^6$ M-1, n = 1.22 for diazepam (correlation coefficient of 0.984), and $K = 1.97 \times 10^6$ M-1 and n = 0.79 for phenylbutazone (correlation coefficient of 0.973), which were comparable with the reported values of 1.02×10^6 M-1 for diazepam (17) and 1.137×10^6 M-1 for phenylbutazone (18).

Validation Studies

The calibration lines were prepared as follows. The HPFA column was removed from the on-line system, and the 5-ml injector loop was then replaced by a 20-μl loop. After washing the extraction column with distilled water for 30 s, 10-μl volumes of a series of standard solutions consisting of 1, 2, 5, 10, and 15 μM L-T4 or D-T4 in methanol was directly injected into the extraction column. After washing the extraction column with distilled water for 30 s, the adsorbed T4 was then back-flushed into the analytical column via the column switching procedure. Finally, the calibration line was prepared by plotting the peak area vs. the injected volume. For the competitive binding study, 10-μl volumes of a series of standard solutions consisting of 10, 20, 40, 60, and 80 μM for L- and/or D-T4, 10, 20, 30, 40, and 50 μM for diazepam, and 5, 10, 20, 40, and 50 μM for phenylbutazone in methanol was injected. All resulting calibration lines showed good linearity (rsq. > 0.999).

The percent recovery of T4 from the extraction column was determined using standard samples at 10, 40, and 80 μM for each enantiomer, and the recoveries of diazepam and phenylbutazone were examined for 5, 20, and 50 μM. The peak-area ratios of three extracted samples were then compared with the unextracted samples to determine the percent recovery. The same three concentrations used for the recovery experiments were used to examine the inter-day and intra-day variability. The accuracy was evaluated by back-calculation and expressed as the percent deviation between the amount found and the amount added for each enantiomer of T4, diazepam, and phenylbutazone for the three concentrations examined. Five samples for each concentration were extracted for each of three consecutive days.

RESULTS AND DISCUSSION

HPFA Profile

For HPFA, it is essential to obtain a plateau region, for which the HPLC conditions including the sample injection volume should be properly optimized. If the injection volume is insufficient or if the elution time of the analyte is too short or long, a clear plateau region cannot be obtained. Figure 3 (A–F) shows each respective HPFA profiles of mixed solution (left), HSA solution (center) and their subtraction chromatogram (right). Clear plateau zones due to unbound L-T4, unbound phenylbutazone and unbound diazepam were observed for the subtraction chromatograms, indicating that the experimental conditions were suitable for the frontal analyses.

Recovery, Accuracy, and Precision

The recoveries for T4 averaged 98% over the 3 concentrations, for diazepam they were 98.8%, and for phenylbutazone they were 97.6%. The accuracy and the intra-day and inter-day variabilities are presented in Table II.

Evaluation of the Binding Parameters

Figure 4 shows the Scatchard plots of the binding between HSA and the T4 enantiomers. Good linearity was observed with a correlation coefficient of 0.983 for both T4 enantiomers, and a contribution from nonspecific binding was not observed. The coefficient of variation (%) for each set of data was below 4.5. Further detailed analysis using nonlinear fitting of the raw data to different binding models incorporating specific and nonspecific binding was performed using Multi software, and from the model regression the optimal AIC values were then compared. The binding parameters were found to be $K = 1.01 \times 10^6$ M-1 and $n = 1.90$ for L-T4, and $K = 9.71 \times 10^5$ M-1 and $n = 1.97$ for D-T4. These results indicate that both enantiomers were bound to HSA at two binding sites with similar affinities.

The total binding affinity for L-T4 of $nK = 1.92 \times 10^6$ M-1 was in agreement with the reported values of $nK = 5.5 \times 10^5$ to 2.5×10^6 M-1 at 37°C (8,10), where Loun and Hage (19) reported that the binding constant for D-T4 of 2.9×10^6 M-1 evaluated using an immobilized HSA column was five times larger than that of L-T4 at 5.7×10^5 M-1. However, distinguishable enantioselectivity was not observed, and one possible reason for this was the change in the binding properties of HSA during the immobilization process.

Identification of the T4 Enantiomer Binding Sites on HSA

Phenylbutazone (site I) and diazepam (site II) were used as the site-specific probes for sites I and II on HSA, respectively, to identify the binding sites of the T4 enantiomers. For this, two series of sample solutions were prepared, where one series contained a constant concentration of 100 μM HSA and 10 μM L- or D-T4 with different concentrations of diazepam or phenylbutazone and the other series contained a constant concentration of 100 μM HSA and a 50 μM diazepam or 50 μM phenylbutazone site-specific probe with different concentrations of L- or D-T4. The unbound concentrations of T4 enantiomer and the site-specific drugs were analyzed using the present system, and the observed data was then compared with the theoretical values, which calculated based on the competitive binding and the independent binding models (20,21).

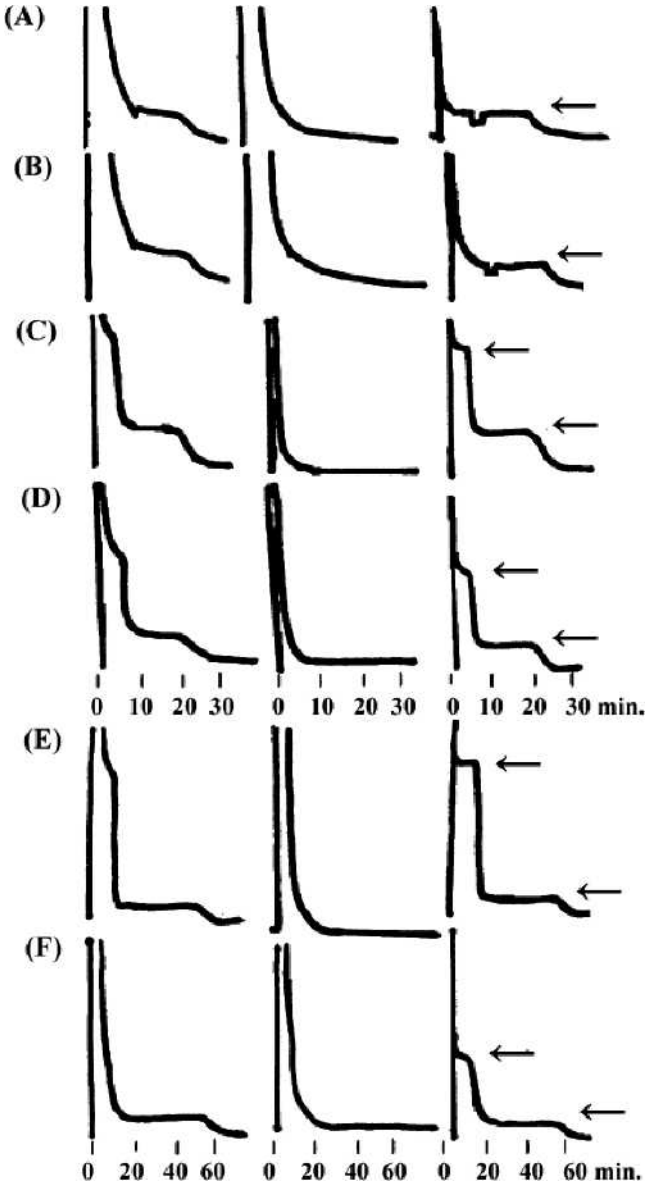

Fig. 3. HPFA profiles (A) 5 μM L-T4 and 100 μM HSA mixed solution (left), 100 μM HSA solution (center), and their subtraction HPFA profile (right). (B) 5 μM D-T4 and 100 μM HSA mixed solution (left), 100 μM HSA solution (center), and their subtraction chromatogram (right). (C) 60 μM L-T4, 50 μM diazepam, and 100 μM HSA mixed solution (left), 100 μM HSA solution (center), and their subtraction chromatogram (right). (D) 40 μM D-T4, 50 μM diazepam, and 100 μM HSA mixed solution (left), 100 μM HSA solution (center), and their subtraction chromatogram (right). Injection volume, 0.8 ml. (E) 20 μM L-T4, 80 μM phenylbutazone, and 100 μM HSA mixed solution (left), 100 μM HSA solution (center), and their subtraction chromatogram (right). (F) 20 μM D-T4, 30 μM phenylbutazone, and 100 μM HSA mixed solution (left), 100 μM HSA solution (center), and their subtraction chromatogram (right). Injection volume, 1.5 ml.

When applying the competitive binding model, it was assumed that:

Table II. Accuracy and Intra- and Inter-day Variabilities for the Assay

	Concentration (μM)	Coefficient variation (%) Inter day (n = 3)	Intra days (n = 15)	Accuracy (%)
L-T4	10	1.4	1.9	98.8
	40	2.2	2.7	99.5
	80	1.0	1.2	99.8
D-T4	10	2.2	2.8	96.8
	40	1.9	1.4	99.4
	80	1.2	2.2	99.2
Diazepam	5	3.9	4.0	98.2
	20	1.0	2.8	99.5
	50	0.6	1.3	99.8
Phenylbutazone	5	2.1	3.1	98.9
	20	2.2	2.4	99.6
	50	2.0	1.8	99.7

i) The binding site number for T4 on HSA molecule was two (n = 2), while that for the site-specific probe was one (n = 1).

ii) T4 and a model drug were competitively bound at one binding site (competitive binding site), while T4, in addition, was bound at another site where the site-specific probe was not bound (non-competitive binding site).

iii) The binding affinity of T4 at the competitive binding site was equal to that at the non-competitive binding site.

For this model, the allosteric effect was not directly taken into consideration, but the allosteric effect, if it was present, could be evaluated as the difference from the theoretical value.

The total concentration for the competitive binding site (P_{1t}) was taken as the sum of the concentrations of the unoccupied site (P_{1u}), the bound concentrations of T4 ($Cb_{(A1)}$), and the site-specific probe ($Cb_{(B)}$) for the competitive binding site and the total concentration for the noncompetitive binding site (P_{2t}) was determined as the sum of the concentration of the unoccupied site (P_{2u}) and the bound concentration of T4 ($Cb_{(A2)}$) for the noncompetitive binding site. Thus,

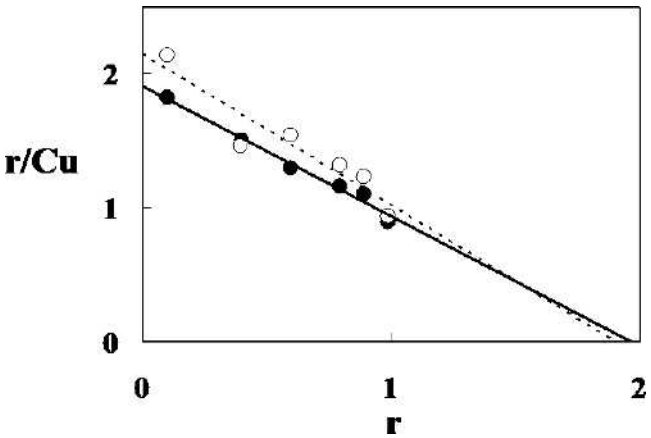

Fig. 4. Scatchard plots of the binding between T4 enantiomers and HSA. Enantiomer: open circles, L-T4; closed circles, D-T4. Broken line and solid line are linear regression lines for L-T4 and D-T4, respectively.

$$P_{1t} = P_{1u} + Cb_{(A1)} + Cb_{(B)} = Pt \quad (2)$$

$$P_{2t} = P_{2u} + Cb_{(A2)} = Pt \quad (3)$$

where Pt represents the concentration for total binding sites.

The total concentration of T4 ($Ct_{(A)}$), the site-specific drug ($Ct_{(B)}$), the binding constant for T4 (K_A) for the competitive binding site, which was assumed to be the same as that for the noncompetitive binding site, and the binding constant for the site-specific probe (K_B) are described by Eqs. (4–8):

$$Ct_{(A)} = Cu_{(A)} + Cb_{(A1)} + Cb_{(A2)} \quad (4)$$

$$Ct_{(B)} = Cu_{(B)} + Cb_{(B)} \quad (5)$$

$$K_A = Cb_{(A1)}/Cu_{(A)}P_{1u} = Cb_{(A2)}/Cu_{(A)}P_{2u} \quad (6)$$

$$K_{B1} = Cb_{(B1)}/Cu_{(B)}P_{1u} \quad (7)$$

where $Cu_{(A)}$ and $Cu_{(B)}$ represent the unbound concentrations of T4 and the site-specific drug, respectively. From these relationships, Eqs. (9–11) can be obtained as:

$$Cu_{(A)} = [K_B Cu_{(B)}\, Pt - (1 + K_B Cu_{(B)})(Ct_{(B)} - Cu_{(B)})]/K_A(Ct_{(B)} - Cu_{(B)}) \quad (8)$$

$$Ct_{(A)} = Cu_{(A)} + K_A Cu_{(A)} Pt[1/(1 + K_A Cu_{(A)} + K_B Cu_{(B)}) + 1/(1 + K_A Cu_{(A)})] \quad (9)$$

$$Cu_{(B)} = K_A Cu_{(A)} Pt/K_B[Ct_{(A)} - Cu_{(A)} - K_A Ct_{(A)}(Pt/1 + K_A Cu_{(A)})] - (1 + K_A Cu_{(A)})/K_B \quad (10)$$

$$Ct_{(B)} = Cu_{(B)} + K_B Cu_{(B)}[Pt/(1 + K_{A1} Cu_{(A)} + K_B Cu_{(B)})] \quad (11)$$

The theoretical values for the unbound concentration were thus calculated from these equations. Theoretical lines were then simulated using Microsoft Excel. Although the number of binding sites (n) for the T4 enantiomers and the site specific probes were assumed to be integers (one or two), the "n" values evaluated by Scatchard analysis were not. Therefore, the corrected K values of 9.57×10^5 M-1, 9.56×10^5 M-1, 1.56×10^6 M-1, and 1.05×10^6 M-1 for L-T4, D-T4, phenylbutazone, and diazepam, respectively, were used for this calculation to not change the total binding affinity (nK values).

For the independent binding model, it is assumed that T4 enantiomer and the site-specific probe were independently bound at different binding sites without any allosteric effect. Cu(A) and Cu(B) were calculated from Eqs. (12 and 13), respectively, where $Pt_{(A)}$ and $Pt_{(B)}$ represent the concentration of total binding sites for the T4 enantiomer and the site specific probe, respectively.

$$K_A Cu_{(A)}^2 + (K_A Pt_{(A)} - K_A Ct_{(A)} + 1)Cu_{(A)} - Ct_{(A)} = 0 \quad (12)$$

$$K_B Cu_{(B)}^2 + (K_B Pt_{(B)} - K_B Ct_{(B)} + 1)Cu_{(B)} - Ct_{(B)} = 0 \quad (13)$$

As shown in Fig. 5, diazepam was used as the site-specific drug. The upper graphs (Fig. 5A) were obtained by increasing the total diazepam concentration up to 90 μM for constant total concentrations of L-T4 and HSA and the lower graphs (Fig. 5B) were obtained by increasing the total L-T4 concentration up to 90 μM for constant total concentrations of diazepam and HSA. The solid line indicates the theoretical values based on the competitive binding model and was calculated as follows. In Fig. 5A ($Ct_{(A)}$ = 10 μM), if an arbitrary value of $Cu_{(A)}$ (e.g., 0.06 μM) was introduced into Eq. (10), $Cu_{(B)}$ was calculated as 16.9 μM. $Ct_{(B)}$was calculated as 0.137

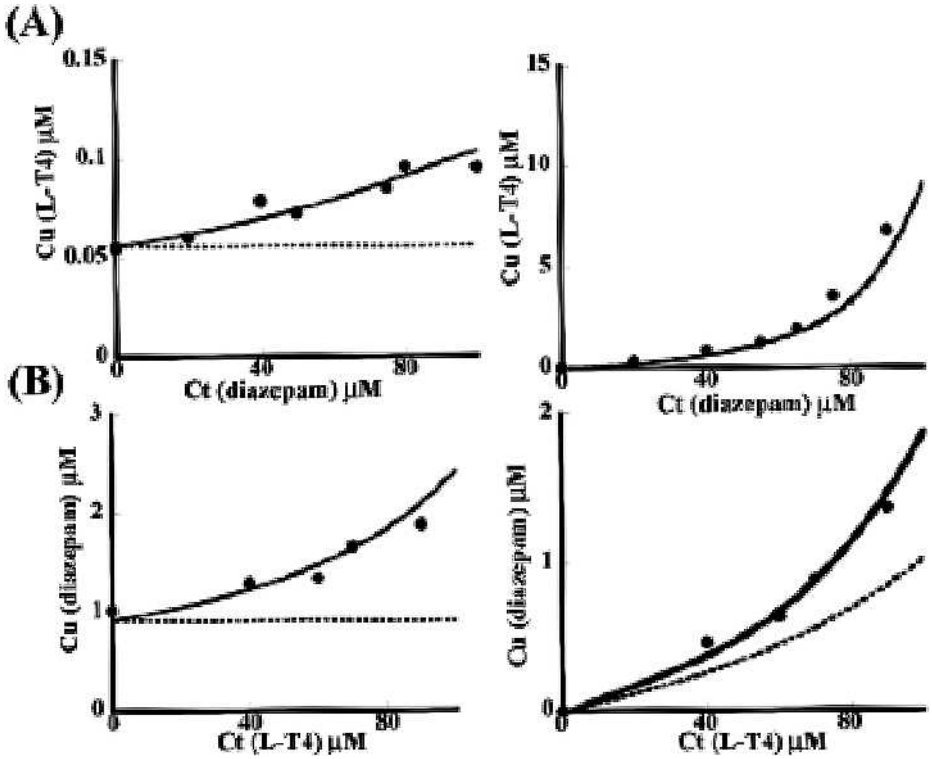

Fig. 5. Competition between L-T4 and diazepam in binding to HSA. Ct and Cu represent the total and unbound drug concentrations, respectively. Sample solutions, (A) 100 μM HSA, 10 μM L-T4 and 0–100 μM diazepam and (B) 100 μM HSA, 50 μM diazepam, and 0–90 μM D-T4. Solid lines: the predicted unbound concentration calculated by assuming that both diazepam and L-T4 are bound competitively to the same site. Broken lines: the predicted unbound concentration calculated by assuming that both diazepam and L-T4 are bound independently to HSA. The closed symbols indicate experimental values.

μM from Eq. (11). A data set of the theoretical values ($Cu_{(A)}$, $Cu_{(B)}$, $Ct_{(B)}$) = (0.06 μM, 16.9 μM, 0.137 μM) was then obtained. Similarly in the case $Cu_{(A)}$ = 0.08 μM, $Cu_{(B)}$ and $Ct_{(B)}$ were calculated as 61.4 μM and 1.05 μM, respectively, and in the case $Cu_{(A)}$ = 0.1 μM, $Cu_{(B)}$ and $Ct_{(B)}$ were calculated as 4.52 μM and 91.1 μM, respectively. In this way, a series of theoretical data sets ($Cu_{(A)}$, $Cu_{(B)}$, $Ct_{(B)}$) was calculated to prepare the theoretical line based on the competitive binding model (solid lines). In Fig. 5B ($Ct_{(B)}$ = 50 μM), an arbitrary value of $Cu_{(B)}$ was introduced into Eq. (8) to calculate $Cu_{(A)}$, and $Ct_{(A)}$ was then calculated from Eq. (9). In this way, a series of theoretical data sets ($Cu_{(B)}$, $Cu_{(A)}$, $Ct_{(A)}$) was calculated to prepare solid line. Broken line indicates the theoretical values based on the independent binding model, and calculated from Eqs. (12 and 13). In every graph, the observed unbound concentrations agreed well with the competitive binding model. These results indicate that L-T4 and diazepam are bound to HSA at the same binding site competitively without a significant allosteric effect.

Figure 6 shows the result when phenylbutazone was used as the site-specific probe. Similarly to Fig. 5, L-T4 and phenylbutazone are bound to HSA at the same binding site competitively without a significant allosteric effect.

The binding sites of D-T4 were identified in the same way. Diazepam was used as the site-specific probe, and phenylbutazone was used (data not shown). In both cases, the observed unbound concentrations agreed with the competitive binding model, indicating that D-T4 is also bound at both sites competitively. These results clearly indicate that both site I and site II are high-affinity binding sites of T4 on HSA, which is consistent with the results of Loun and Hage (19).

Enantiomer-Enantiomer Interaction upon T4-HSA Binding

In many cases, a pair of enantiomers were competitively bound to the protein at the same site. It was therefore important to clarify the effect of enantiomer-enantiomer interactions upon T4-HSA binding. Two series of sample solutions were prepared and analyzed using the HPFA-chiral HPLC system for this purpose. One series of sample solutions consisted of 100 μM HSA, 40 μM D-T4, and different concentration of L-T4 ranging between 0 and 80 μM, and the other series contained 100 μM HSA, 40 μM L-T4, and different concentrations of D-T4 ranging between 0 and 80 μM. The measured unbound concentrations were then compared with the theoretical values that were calculated based on the competitive and independent binding models.

For the competitive binding model, it was assumed that one enantiomer was bound to HSA at two binding sites with the same binding affinities of n = 2, K = 9.57×10^5 M-1 for L-T4, and n = 2, K = 9.56×10^5 M-1 for D-T4. The unbound concentrations of D-T4 and L-T4, $Cu_{(D)}$ and $Cu_{(L)}$, respectively, were calculated using the following equations,

$$Ct_{(L)} = Cu_{(L)} + K_{(L)}Cu_{(L)}nPt/(1 + K_{(L)}Cu_{(L)} + K_{(D)}Cu_{(D)}) \quad (14)$$

$$Ct_{(D)} = Cu_{(D)} + K_{(D)}Cu_{(D)}nPt/(1 + K_{(D)}Cu_{(D)} + K_{(L)}Cu_{(L)}) \quad (15)$$

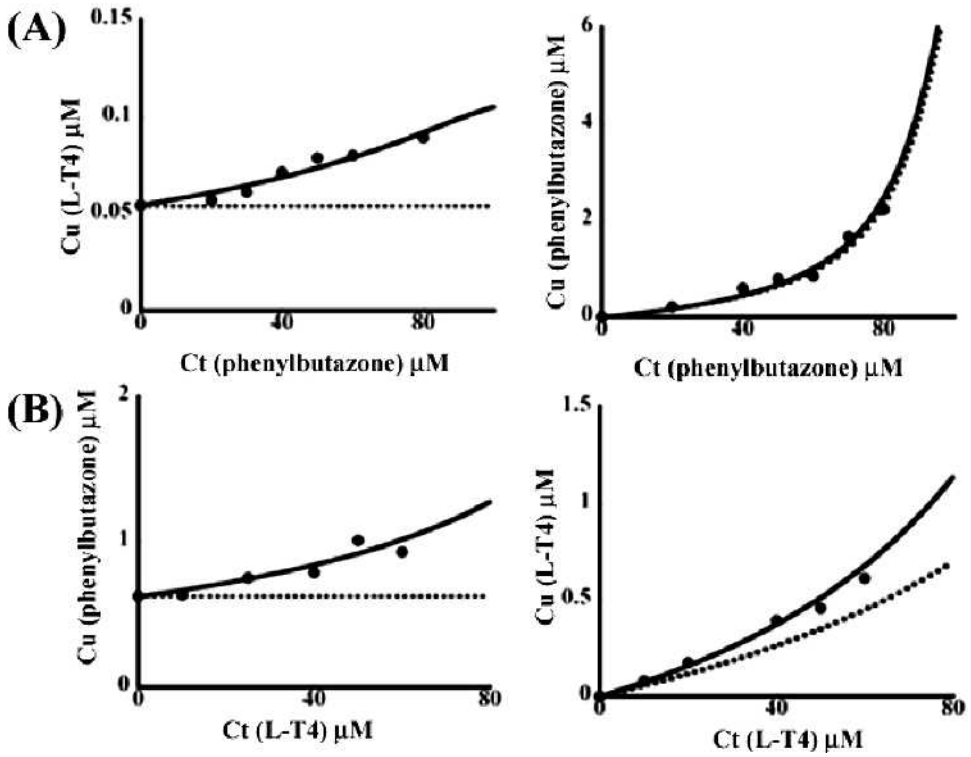

Fig. 6. Competition between L-T4 and phenylbutazone in binding to HSA. Ct and Cu represent the total and unbound drug concentrations, respectively. Sample solutions, (A) 100 μM HSA, 10 μM L-T4, and 0–80 μM phenylbutazone and (B) 100 μM HSA, 50 μM phenylbutazone and 0–60 μM T4. Solid lines: the predicted unbound concentration calculated by assuming that both phenylbutazone and L-T4 are bound competitively to the same site. Broken lines: the predicted unbound concentration calculated by assuming that both phenylbutazone and L-T4 are bound independently to HSA. The closed symbols indicate experimental values.

$$Cu_{(L)} = K_{(D)}Cu_{(D)}nPt/K_{(L)}\,(Ct_{(D)} - Cu_{(D)}) - (1 + K_{(D)}Cu_{(D)})/K_{(L)}) \quad (16)$$

$$Cu_{(D)} = K_{(L)}Cu_{(L)}nPt/K_{(D)}\,(Ct_{(L)} - Cu_{(L)}) - (1 + K_{(L)}Cu_{(L)})/K_{(D)} \quad (17)$$

where K_L and K_D are the binding constants for L-T4 and D-T4, respectively.

For the independent binding model, it is assumed that both enantiomers were independently bound at different binding sites without any allosteric effect. $Cu_{(L)}$ and $Cu_{(D)}$ were calculated from Eqs. (18 and 19), which are essentially the same as Eqs. (12 and 13)

$$K_D Cu_{(D)}^2 + (K_D Pt_{(D)} - K_D Ct_{(D)} + 1)Cu_{(D)} - Ct_{(D)} = 0 \quad (18)$$

$$K_L Cu_{(L)}^2 + (K_L Pt_{(L)} - K_L Ct_{(L)} + 1)Cu_{(L)} - Ct_{(L)} = 0 \quad (19)$$

where $Pt_{(L)}$ and $Pt_{(D)}$ represent the total binding site concentrations for L-T4 and D-T4, respectively.

Figure 7 shows the measured and theoretical unbound concentrations. Figure 7A indicates the results when the total concentration of L-T4 was increased while the total concentrations of D-T4 and HSA were constant. Figure 7B was obtained when the total concentration of D-T4 was increased while those of L-T4 and HSA were constant. The solid lines indicate the theoretical values calculated based on the competitive binding model, and were prepared as follows. In Fig. 7A ($Ct_{(D)}$ = 40 μM), an arbitrary value for $Cu_{(D)}$ was introduced into Eq. (16) to calculate $Cu_{(L)}$, and $Ct_{(L)}$ was calculated from Eq. (14). Thus, a series of theoretical values ($Cu_{(D)}$, $Cu_{(L)}$, $Ct_{(L)}$) were calculated to produce the theoretical line. In Fig. 7B ($Ct_{(L)}$ = 40 μM), an arbitrary value for $Cu_{(L)}$ was introduced into Eq. (17) to calculate $Cu_{(D)}$, and $Ct_{(D)}$ was calculated from Eq. (15). A series of theoretical values ($Cu_{(L)}$, $Cu_{(D)}$, $Ct_{(D)}$) was then calculated to produce the theoretical line. The broken lines indicate the theoretical values based on the independent binding model, which were prepared from Eqs. (18 and 19).

For both sample sets, the observed data agreed well with the solid lines. These results indicate that L-T4 and D-T4 were bound to HSA at the same two binding sites, which were identified as sites I and II, and that the pairs of enantiomers competed for both binding sites. No significant allosteric effect was observed.

Conventional methods used to determine unbound concentrations such as ultrafiltration and equilibrium dialysis are difficult to directly connect to a chiral separation process. In contrast, HPFA can be directly coupled with a chiral HPLC system, enabling simple, easy and precise binding analysis of enantiomeric pairs. This is one advantage of the HPFA method for enantioselective binding studies. Binding analysis involving the use of an on-line HPFA-chiral HPLC system followed by comparisons with theoretical models is a versatile approach for investigating enantiomer-enantiomer interactions.

The current study found that the HPFA method is a useful tool for the study of biomolecular interactions.

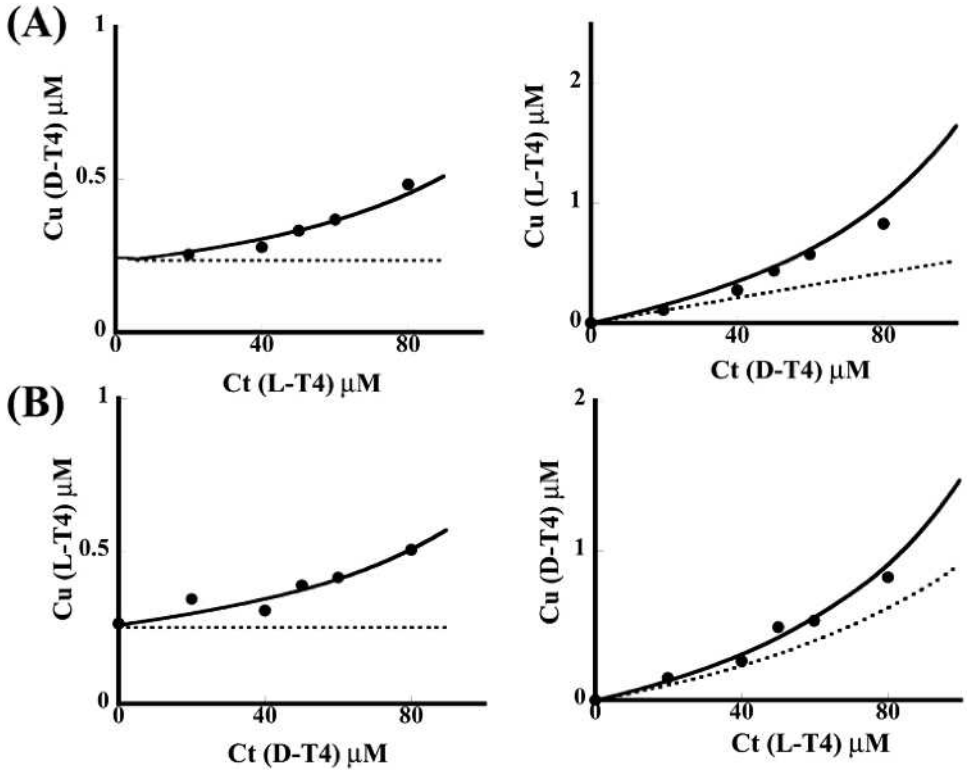

Fig. 7. Competition between T4 enantiomers in binding to HSA. Ct and Cu represent the total and unbound T4 concentrations, respectively. Sample solutions, (A) 100 μM HSA, 40 μM D-T4, and 0–80 μM L-T4 and 100 μM HSA, (B) 40 μM L-T4 and 0–80 μM D-T4. Solid lines: the predicted unbound concentration calculated by assuming that both D- and L-T4 are bound competitively to the same site. Broken lines: the predicted unbound concentration calculated by assuming that both D- and L-T4 are bound independently to HSA. The closed symbols indicate experimental values.

ACKNOWLEDGMENTS

This research was supported by the 21st Century Center of Excellence Program "Knowledge Information Infrastructure for Genome Science" from the Japan Society for the Promotion of Science.

REFERENCES

1. S. C. Chattoraj, N. B. Watts, and N. W. Trietz. *Textbook of Clinical Chemistry*, Saunders, Philadelphia, 1986, pp. 1116–1138.
2. S. Refetoff, P. R. Larsen, L. J. DeGroot, G. M. Besser, G. F. Cahill, and E. Steinberger. *Endocrinology*, Vol. 1, 2nd ed., Saunders, Philadelphia, 1989, Ch. 38.
3. S. Pannain, M. Feldman, U. Eiholzer, R. E. Weiss, N. H. Scherberg, and S. Refetoff. Familial dysalbuminemic hyperthyroxinemia in a swiss family caused by a mutant albumin (R218P) shows an apparent discrepancy between serum concentration and affinity for thyroxine. *J. Clin. Endocrinol. Metab.* **85**:2786–2792 (2000).
4. L. D. Mechtol and W. I. Warner. Dextrothyroxine for lowering serum cholesterol. Analysis of data on 6066 patients. *Angiology* **20**:565–579 (1969).
5. P. Starr. Depression of the serum cholesterol level in myxedematous patients by an oral dosage of sodium dextro-thyroxine which has no effct on the basal metabolic rate or electrocardiogram. *J Clin Endocr.* **20**:116–119 (1960).
6. M. Hunfner. Influence of D-thyroxine on plasma thyroid hormone levels and TSH secretion. *Horm. Metab. Res.* **9**:69–73 (1977).
7. A. Ishihara, S. Sawatsubashi, and K. Yamauchi. Endocrine disrupting chemicals: interference of thyroid hormone binding to transthyretins and to thyroid hormone receptors. *Mol. Cell. Endocrinol.* **31**:105–117 (2003).
8. M. Tabachnick. Thyroxine – protein interactions. Binding of thyroxine to human serum albumin and modified albumins. *J. Biol. Chem.* **239**:1242–1249 (1964).
9. R. F. Steiner, J. Poth, and J. Robbins. The binding of thyroxine by serum albumin as measured by fluorescence quenching. *J. Biol. Chem.* **541**:560–567 (1966).
10. G. L. Tritsch, C. E. Ratheke, and C. M. Weiss. Thyroxine binding by human serum albumin. *J. Biol. Chem.* **236**:3163–3167 (1961).
11. M. Tabachnick. Thyroxine – protein interactions. Thermodynamic values for the association of thyroxine with human serum albumin. *J. Biol. Chem.* **242**:1646–1650 (1967).
12. B. Loun and D. S. Hage. Characterization of thyroxine-albumin binding using high-performance affinity chromatography. I. Interactions at the warfarin and indole sites of albumin. *J. Chromatogr.* **579**:225–235 (1992).
13. A. Shibukawa and T. Nakagawa. High-performance frontal analysis for drug-protein binding study. *J. Pharm. Biomed. Anal.* **18**:1047–1055 (1999).
14. E. Rodriguez Rosas, A. Shibukawa, K. Ueda, and T. Nakagawa. Enantioselective protein binding of semotiadil and levosemotiadil determined by high-performance frontal analysis. *J. Pharm. Biomed. Anal.* **15**:1595–1601 (1997).
15. M. E. Rodriguez Rosas, A. Shibukawa, Y. Yoshikawa, Y. Kuroda, and T. Nakagawa. Binding study of semotiadil and levosemotiadil with alpha(1)-acid glycoprotein using high-performance frontal analysis. *Anal. Biochem.* **274**:27–33 (1999).
16. A. Shibukawa, A. Terakita, and T. Nakagawa. High-performance frontal analysis-high-performance liquid chromatographic system for stereoselective determination of unbound ketoprofen enantiomers in plasma after direct sample injection. *J. Pharm. Sci.* **81**:710–715 (1992).
17. H. Yuan and J. Pawliszyn. Application of solid-phase microex-

traction in the determination of diazepam binding to human serum albumin. *Anal. Chem.* **73**:4410–4416 (2001).
18. T. Kosa and M. Otagiri. Species differences of serum albumins: I. Drug binding sites. *Pharm. Res.* **14**:1607–1612 (1997).
19. B. Loun and D. S. Hage. Characterization of thyroxine-albumin binding using high-performance affinity chromatography 2. Comparison of binding of thyroxine, triiodothyronines and related compounds at the warfarin and indole sites of human serum albumin. *J. Chromatogr. B* **665**:303–314 (1995).
20. A. Shibukawa, N. Ishizawa, T. Kimura, T. Nakagawa, and I. W. Wainer. Plasma protein binding study of oxybutynin by high-performance frontal analysis. *J. Chromatogr. B* **768**:177–188 (2002).
21. A. Shibukawa, Y. Yoshikawa, T. Kimura, T. Nakagawa, and I. W. Wainer. Binding study of desethyloxybutynin using high-performance frontal analysis method. *J. Chromatogr. B* **768**:189–197 (2002).